



HAL
open science

Post midnight spread-F occurrence over Waltair (17.7° N, 83.3° E) during low and ascending phases of solar activity

K. Niranjana, P. S. Brahmanandam, P. Ramakrishna Rao, G. Uma, D. S. V. V. D. Prasad, P. V. S. Rama Rao

► To cite this version:

K. Niranjana, P. S. Brahmanandam, P. Ramakrishna Rao, G. Uma, D. S. V. V. D. Prasad, et al.. Post midnight spread-F occurrence over Waltair (17.7° N, 83.3° E) during low and ascending phases of solar activity. *Annales Geophysicae*, 2003, 21 (3), pp.745-750. hal-00317019

HAL Id: hal-00317019

<https://hal.science/hal-00317019>

Submitted on 18 Jun 2008

HAL is a multi-disciplinary open access archive for the deposit and dissemination of scientific research documents, whether they are published or not. The documents may come from teaching and research institutions in France or abroad, or from public or private research centers.

L'archive ouverte pluridisciplinaire **HAL**, est destinée au dépôt et à la diffusion de documents scientifiques de niveau recherche, publiés ou non, émanant des établissements d'enseignement et de recherche français ou étrangers, des laboratoires publics ou privés.

Post midnight spread-F occurrence over Waltair (17.7° N, 83.3° E) during low and ascending phases of solar activity

K. Niranjana, P. S. Brahmanandam, P. Ramakrishna Rao, G. Uma, D. S. V. V. D. Prasad, and P. V. S. Rama Rao

Department of Physics, Andhra University, Visakhapatnam 530 003, India

Received: 6 May 2002 – Revised: 5 September 2002 – Accepted: 20 September 2002

Abstract. A study carried out on the occurrence of post midnight spread-F events at a low-latitude station, Waltair (17.7° N, 83.3° E), India revealed that its occurrence is maximum in the summer solstice months of the low solar activity period and decreases with an increase in the sunspot activity. The F-region virtual height variations show that 80% of these spread-F cases are associated with an increase in the F-region altitude. It is suggested with the support of the night airglow 6300 Å zenith intensity data obtained with co-located ground-based night airglow photometer and electron temperature data from the Indian SROSS C2 satellite that the seasonal variation of the occurrence and probable onset times of the post midnight spread-F depend on the characteristics of the highly variable semipermanent equatorial Midnight Temperature Maximum (MTM).

Key words. Ionosphere (ionospheric irregularities; ionosphere atmosphere interactions) Atmospheric composition and structure (airglow and Aurora)

1 Introduction

It is established from various diagnostic techniques that Equatorial Spread-F (ESF) irregularities occur over a wide range of scale sizes and that no single instability mechanism could account for such a variety of scale sizes. Also, it is known that the causative mechanism for the incidence/suppression of the otherwise susceptible plasma for the occurrence of the spread-F are different for the pre- and post midnight periods, in view of the ambient conditions that prevail in the respective parts of the night. There are many reports on the morphology of ionogram ESF which include the solar cycle, season, and geomagnetic activity related variations at specific locations around the globe. A distinctive feature of the incidence of spread-F on ionograms in the Indian sector is the solar activity dependent seasonal behaviour.

Subba Rao and Krishna Murthy (1994) investigated the occurrence of spread-F at Trivandrum, India on a seasonal basis during both the solar epochs and interpreted the seasonal behaviour in terms of the Rayleigh Taylor instability growth mechanism. During the high solar activity epochs, the occurrence of spread-F is maximum in the post sunset periods and is more probable during the equinox season than during the solstice. During summer solstice of low solar activity period, the peak occurrence is seen in the post midnight hours preceded by an abnormal increase in the F-region height. A pre-sunrise peak in the occurrence of spread-F is reported in the Brazilian sector at solar minimum (MacDougall et al., 1998).

It is generally accepted that the generalized Rayleigh Taylor (RT) instability mechanism is responsible for the generation and growth of spread-F irregularities. Spread-F occurrence at equatorial stations is associated with post sunset height rise in the F-region (Chandra and Rastogi, 1972). The high altitude of the F-region, where collision frequencies are low, is favourable for the growth of the irregularities by the RT instability mechanism. The pre-midnight growth rates are higher during the sunspot maximum compared to those during post midnight periods, leading to a positive correlation of equatorial spread-F with solar activity. Abdu et al. (1992) pointed out that the height gradient of vertical drift also plays an important role in the occurrence of spread-F. Maruyama and Matuura (1984) in an attempt to account for seasonal longitude ESF occurrence rates, suggested the ability of trans-equatorial neutral winds to inhibit the ESF activity. Mendillo et al. (1992) suggested that a neutral wind driven mechanism should act with equivalent efficiency on a night-by-night basis and even within a given evening. They suggested that the nightly requirements for the RT instability growth leading to the incidence of ESF are: post sunset rise of F-region, availability of seed perturbation to launch the RT mechanism and an absence of a strong trans-equatorial thermospheric wind. Maruyama (1988) with a diagnostic model for ESF, reported that a trans-equatorial wind and the $\mathbf{E} \times \mathbf{B}$ drift are equally important in controlling the generation of ESF.

Correspondence to: K. Niranjana
(niranjankandula@hotmail.com)

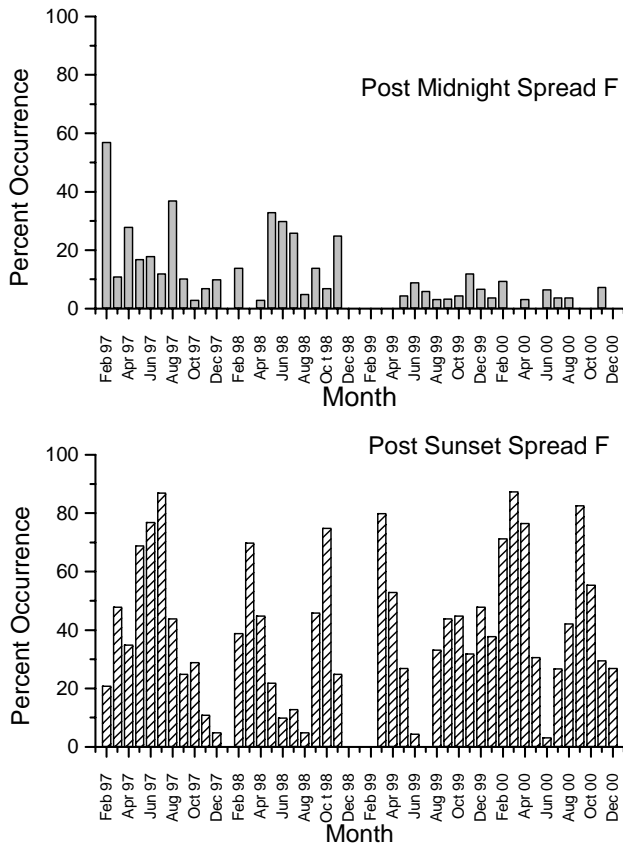


Fig. 1. Histogram showing the monthly percent occurrence of post midnight spread-F (top panel) and post sunset spread-F (bottom panel) at Waltair during 1997–2000.

Raghava Rao et al. (1992) with nonlinear numerical modeling, suggested that vertical downward winds in the ambient gas have the potential to cause the ESF bubble phenomenon, while an upward wind could inhibit the same. Mendillo et al. (2001) from a multi-technique approach reported that the best available pre-cursor for pre-midnight ESF appears to be the strength of the electrodynamically driven Appleton anomaly pattern at sunset and that the correlative studies of the ESF activity and magnitude of meridional winds afford no convincing evidence of the wind suppression mechanism.

In the Indian sector, spread-F conditions during the low sunspot period are known to develop during the post midnight periods of the summer solstice months. The occurrence is associated with a distinct height rise in the F-layer. Secondly, the post midnight occurrence of the spread-F over a location may not be entirely due to the instabilities in the local plasma, but could be due to the passage of fossil plumes generated elsewhere along the terminator and could move in the direction of the observing station. Sastri (1999) from an investigation of the ionograms data from a dip equatorial station in Kodaikanal (India) reported that the F-layer height does not play a pivotal role in the midnight onset of spread-F during the summer solstice months of solar minimum.

Even after such extensive investigations on the ambient

conditions during the onset and growth of the spread-F irregularities, there still remain some uncertainties about the conditions that favour the incidence of spread-F, demanding more efforts in the understanding of the spread-F phenomenon at different locations. In view of this, an attempt is made to identify the ambient conditions that favour the appearance of localized post midnight irregularities causing spread-F in ionograms.

2 Data and methodology

Waltair (17.7° N, 83.3° E) is a low-latitude station in India located in the transition zone between the equator and the Appleton anomaly crest region. The station is equipped with an IPS 42 Digital ionosonde system and a tilting filter night airglow photometer. The ionograms data pertaining to the low and ascending solar activity period 1997–2000 has been used for identifying the post midnight spread-F events without any spread-F occurrence during the pre-midnight periods and the associated variations of the F-region virtual height. The night airglow 6300 Å zenith intensity data is used to evaluate the mean characteristics of the midnight temperature maximum (as seen by the brightness wave properties) that could effect the incidence of spread-F in otherwise susceptible F-region plasma. The support of in situ electron temperature measurements of the RPA on board the Indian SROSS C2 satellite is taken in evaluating the probable time of occurrence of the semipermanent midnight temperature maximum.

3 Occurrence of post midnight spread-F

From an examination of the ionograms for the period from February 1997 to December 2000, it is observed that the post midnight spread-F occurrence is maximum during the summer solstice months (May, June, July and August) of the low solar activity period. The post midnight occurrence shown in light gray in the top panel of Fig. 1 decreased as the solar activity increased from 1997 to 2000 and was minimum in the year 2000. The post sunset spread-F occurrence, however, increased with solar activity (bottom panel of Fig 1). This is in conformity with the results reported by Abdu et al. (1992) in the Brazilian sector and by Subba Rao and Krishna Murthy (1994) for the Indian equatorial station Thumba. However, during 1997 and 1998, the post midnight occurrence was almost equally probable, with marginally higher probability during 1998. It has been observed that the most probable time for the occurrence of post midnight spread-F at Waltair during the summer solstice months is between 01:00 to 03:00 IST and not before 01:00 IST.

The nocturnal variation of the F-region virtual height $h'F$ (solid line) on two typical days in summer solstice when the post midnight spread-F was observed at Waltair is shown in Fig. 2. The points with vertical bars show the mean magnetically quiet non-spread-F day (neither pre- nor post midnight) nocturnal variation of $h'F$ during that month, along with the standard deviation. The horizontal solid line represents the

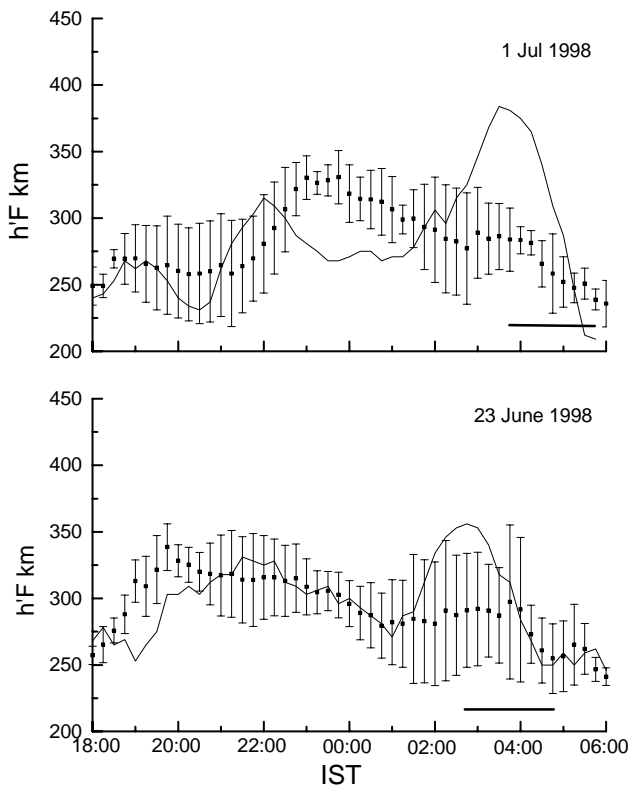


Fig. 2. Nocturnal variation of the F-layer virtual height ($h'F$) on two typical post midnight spread-F days during the summer solstice months. The points show the mean F-layer height of magnetically quiet non spread-F days and the vertical line shows the standard deviation. The horizontal solid line indicates the presence of spread-F on ionograms.

presence and duration for which spread-F is present on the ionograms. It is evident that before the onset of spread-F, the F-layer is lifted to higher altitudes making the conditions favourable for the incidence of spread-F. In majority of the cases, the condition of the high altitude F-region ionosphere is satisfied before the onset of spread-F. However, in some cases, post midnight spread-F is seen even without any rise in the F-region altitude. In such cases, the spread-F is seen many times with a few sequences of ionograms showing spread-F and intermediate sequences without spread-F. The spread-F seen in such cases with no F-region altitude rise resemble the drifting fossil plumes generated at the sunset terminator to the west of the present location and are seen drifting eastward.

One point of interest in Fig. 2 is the descent of the F-layer from 22 h showing a minimum height around local midnight. This feature is seen in both the cases presented in Fig. 2 and is a more general observation during summer solstice. Thereafter, the F-region is lifted to higher altitudes, making the conditions favourable for the growth of the RT instability mechanism leading to the onset of spread-F. However, during the winter solstice months, the midnight descent of the F-layer is delayed, starts around or after local midnight (Fig. 3)

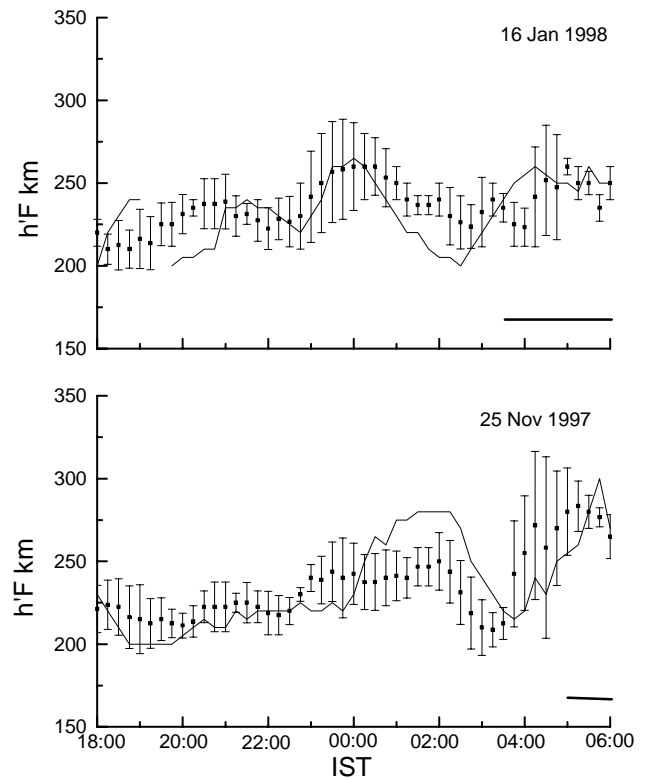


Fig. 3. Same as in Fig. 2 for two typical post midnight spread-F days in winter solstice.

and continues up to 02:00–03:00. Later, the F-region altitude rises before the onset of spread-F. Thus, the onset of post midnight spread-F during this season is seen at a later time compared to the summer solstice months.

Table 1 gives the statistical details of all the post midnight spread-F events over Waltair considered in the present study. It may be noticed that in most of the cases the onset of post midnight spread-F is associated with an increase in the F-region altitude. The most probable time of onset of spread-F is between 01:00 to 03:00 during the summer solstice months with low sunspot activity period, while it is delayed by an hour or two during the winter solstice months. For the cases which were not associated with an altitude increase of the F-region, the probable times of occurrence were found to be around midnight.

4 Features of MTM observed over the location

The variation of 630 nm night airglow zenith intensity over Waltair on two typical nights during the summer solstice months of 1997–1998 (top panel) when the brightness wave representing the semipermanent midnight temperature maximum is present is shown in Fig. 4. The maximum intensity representing the MTM (on days when it is present), which is strongest during this season, is observed around 00:00 to 01:00 IST, where as during the winter solstice months,

Table 1. Statistical details of post midnight spread-F events

| Season and year | No. of cases | No. of cases which show F-layer altitude increase before the onset of spread-F | Most probable onset times IST | No. of cases which show downward movement in F-region altitude around/after 00:00 IST |
|----------------------|--------------|--|-------------------------------|---|
| 1997 Summer solstice | 14 | 12 | 01:00–03:00 | 14 |
| 1998 Summer solstice | 18 | 14 | 01:30–03:30 | 9 |
| 1999 Summer solstice | 7 | 5 | 02:00–04:00 | 2 |
| 2000 Summer solstice | 4 | 2 | 02:00–04:30 | 3 |
| 1997 Winter solstice | 11 | 6 | 02:00–04:30 | 4 |
| 1998 Winter solstice | 4 | 3 | 03:00–04:00 | 2 |
| 1999 Winter solstice | 7 | 4 | 01:45–03:15 | 5 |
| 2000 Winter solstice | 3 | 2 | 02:45–06:30 | 2 |

it is seen with less prominence and at a later time (01:00–03:00 IST), as seen in the bottom panel.

The contour maps of F-region electron temperature derived from RPA data on board the Indian SROSS C2 satellite for the years 1997–1998 are shown in Fig. 5. The bottom panel corresponds to the summer solstice months and the top panel to the winter solstice months. The satellite altitude for these measurements was between 450–550 km when these measurements were made. However, the conditions at these altitudes, by and large, depend on the ambient ionospheric conditions. It may be seen from Fig. 5 that during the summer solstice months, there is a significant temperature gradient from about 1050° K at the equatorial and lower latitudes, to about 900° K around the latitudes of Waltair (14–18° N) from 22:00 to 24:00 IST. As the time progresses, in the early hours there is practically no temperature gradient as a function of latitudes from 01:00 IST onwards. In contrast, during the winter solstice months, while there is no defined temperature gradient during the 22:00 to 24:00 IST, the diurnal decrease of temperature is seen at all latitudes. But, between 01:00 to 03:00 IST latitude, a gradient in temperature is seen from equatorial (1050° K) to lower latitudes (900° K), although not as significant as the one seen in the June solstice around local midnight. Though there is a definite temperature difference between the equatorial and low-latitudes, the temperature gradients seen are not very well defined. Thus, the brightness features observed in the night airglow zenith intensities resemble the brightness wave characteristics associated with MTM, as reported by Colerico et al. (1996) and coincide with the temperature enhancements that reflect the semipermanent midnight temperature maximum (MTM) in the in situ data of the SROSS C2 satellite.

5 Discussion

After sunset, the regular E-region ionosphere begins to recombine and there is effectively no E-region to short out any irregularities in the F-region. Owing to the recombination and possible $\mathbf{E} \times \mathbf{B}$ drifts due to the polarization electric fields, the bottom side F-region begins to steepen. When the

altitude of the F-region is high enough to overcome the recombination effects, as in the post sunset cases during moderate to high sunspot activity periods, plasma density fluctuations begin to grow on the bottom side via the RT instability mechanism. These irregularities, in turn, form plasma density depletions (bubbles) on the bottomside, which, in turn, rise nonlinearly to topside. These steepening bubbles can bifurcate to form small-scale structures by a cascade or two step mechanism (Ossakow, 1981). Subba Rao and Krishna Murthy (1994) reported that in the generalized RT instability mechanism, the growth rate could be due to the combined effects of the gravitational and cross field instability, and that these terms closely follow the layer height and become higher when the layer height is around 300 km and above. It is generally accepted that the primary mechanism for the growth of instability is a high altitude F-region where collision frequencies are low. The growth rates follow $h'F$ variations and the pre-midnight growth rates are high in sunspot maximum compared to sunspot minimum years. Once developed, the irregularities move depending on the prevailing neutral wind and thus, an eastward wind can cause the bubbles to move westward with respect to the bulk plasma motion.

Thus, the absence of spread-F on a given night, with the preconditions of higher altitude F-region and steep plasma gradients satisfied, could be due to the suppression of the instability growth rates by various factors. Thus, the periods of no ESF development must be associated with factors that inhibit the otherwise susceptible ionosphere to instability growth. It is reported that the trans-equatorial wind plays a pivotal role in the suppression of the RT growth rate and that the wind effect is more prominent if the $\mathbf{E} \times \mathbf{B}$ drift reversal time is late (Maruyama, 1988) during the post sunset periods. Abdu et al. (1992) reported that small angles between sunset terminator and magnetic meridian favour the post sunset ESF development. Perfect alignment of the terminator with magnetic meridian tends to decrease the efficiency of ESF development. Normally in a given longitude sector, ESF occurs when the sunset terminator is approximately aligned to the geomagnetic flux tube. Under such conditions, thermo-

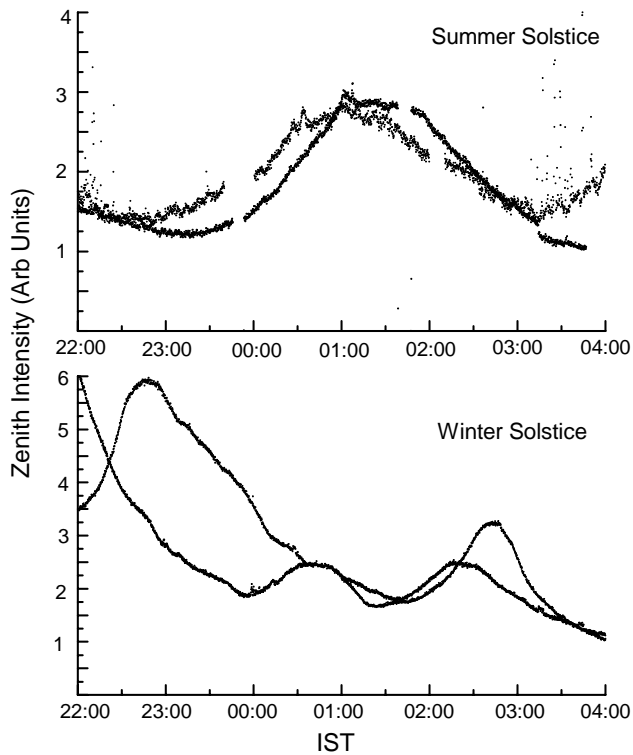


Fig. 4. Nocturnal variation of airglow zenith intensity on two typical days showing the brightness wave feature during summer solstice (top panel) and winter solstice (bottom panel).

spheric winds typically have a small component along the meridian and thus suppression of the RT instability on the average is unlikely. Since the trans-equatorial component of the thermospheric wind in the magnetic plane is determined by the magnetic declination angle, the magnetic declination effect of ESF may also be well explained by the wind effect. Thus, a nightly requirement for the development of ESF is the absence of the trans-equatorial wind, in addition to the increase in the height of the F-layer and the electron density gradient.

In addition, vertical winds also control the RT growth rates (Raghava Rao et al., 1992). A downward wind pushing the F-region into lower altitudes of higher recombination rates does favours the RT growth rate, while an upward wind acts otherwise. It is also well known that thermospheric neutral wind speed is determined not only by the global circulation due to solar forcing, but also by the semipermanent equatorial Midnight Temperature Maximum (MTM) (Herraro et al., 1993), particularly with reference to the mechanisms operative around and after local midnight. MTM is strongest in summer solstice of solar minimum and its characteristics like the amplitude and time of maximum occurrence are variable from day to day. Therefore, day-to-day variability in the neutral wind could impose a corresponding variability in the development of ESF.

The data presented here pertains to the post midnight onset of spread-F. It is to be noted that the onset of post midnight

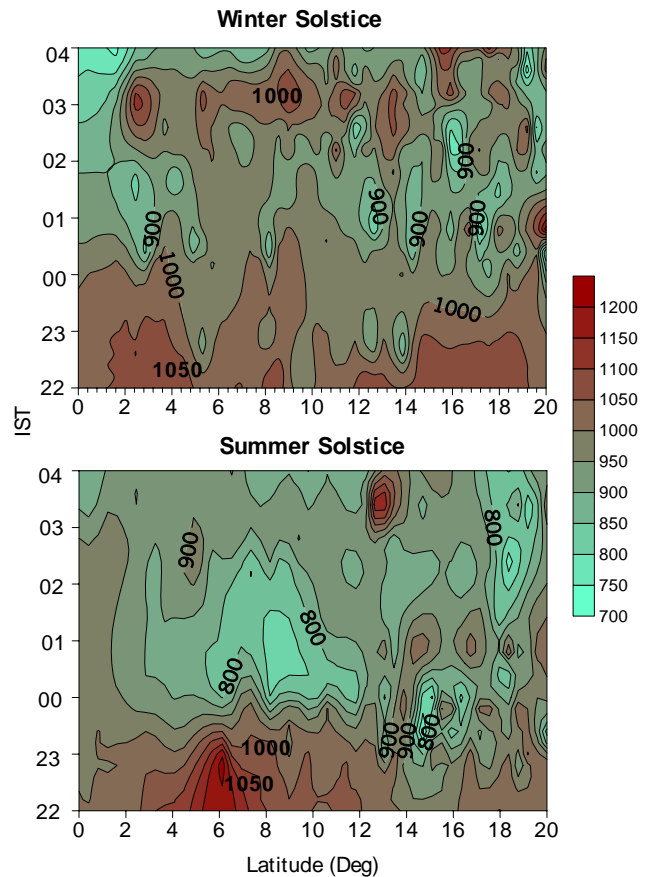


Fig. 5. Isothermal contours of electron temperature derived from the SROSS C2 RPA data for summer solstice months (bottom panel) and winter solstice months (top panel) during 1997–1998.

spread-F in 80% of the cases is preceded by a sharp increase in the F-region altitude, satisfying the base level condition of the high F-region altitude that favours the growth of the RT instability mechanism. However, on some days, spread-F was observed even without a height rise, either prior to the onset or after the onset of spread-F. During these nights, the spread-F activity was mostly of a recurrent short duration type and could possibly be of a non-local origin. This ESF activity is believed to be due to the irregularities generated at the terminator, moving westward and seen during post midnight periods over Waltair. Such spread-F is observed to be very intense and patchy in character.

The post midnight spread-F, when viewed as a function of the onset times, appears earlier during the summer solstice months, while during winter solstice the occurrence is delayed. The characteristics reflected in the night airglow observations and the RPA electron temperature data presented above indicate that the semipermanent equatorial midnight temperature maximum is strongest and occurs around local midnight during the summer solstice of low and ascending solar activity period. In winter solstice months it is delayed in time. Colerico et al. (1996) have also observed frequent enhancements in 6300 Å Airglow emissions, which

they referred to as the Midnight Brightness Wave (MBW) and concluded that this enhancement is a signature of the thermospheric Midnight Temperature Maximum, a large-scale, highly variable neutral temperature anomaly. During the nighttime, the electron temperature is equal to the ion temperature and hence, can be considered to represent the neutral temperature. The SROSS C2 data, pertaining to the topside F-region, indicates the presence of a strong temperature enhancement at the equatorial latitudes in summer solstice. Though highly variable in nature, the MTM has a statistical consistency in the time of occurrence and hence, is seen clearly in the isothermal contours presented in Fig. 5 as a function of latitude and time. The MTM is accompanied by a pressure bulge which significantly modifies the meridional neutral winds (Herrero and Meriwether, 1980). This pressure variation could lead to a reversal/abatement in the neutral wind from the equator to poleward, which, in turn, could lower the F-region at lower latitudes (as shown in h/F variations in Figs. 2 and 3) to produce an increase in the 6300 Å airglow intensities.

In summer solstice months, as the MTM occurs around midnight, the effect of the temperature variations cease by around 01:00 IST and hence, the poleward wind set in by the MTM ceases by 01:00 IST as seen in the SROSS C2 temperature data and the airglow intensities. Thus, the F-region altitude rise is not effected after 01:00 IST in the summer solstice months at lower latitudes. Therefore, an increase in the F-region altitude makes the conditions favourable for the growth of RT instability mechanism (Subba Rao and Krishna Murthy, 1994) leading to the onset of spread-F even by 01:00 IST in summer solstice.

However, during winter solstice months of low sunspot activity period, the MTM is delayed in time and continues to effect the meridional neutral winds until about 02:00 IST. Therefore, the lowering of the F-region altitude as a consequence of the pressure bulge due to MTM continues well beyond 02:00 LT (Fig. 3). Hence, the F-region altitude increase is inhibited, making the conditions unfavourable for the growth of the RT instability and hence, the onset of the post midnight spread-F is delayed in the December solstice months. Secondly, due to the highly variable nature of MTM, on some occasions it may continue up to even later hours and by the time the MTM induced neutral wind perturbation diminishes, the ionization level may come well below the threshold level for any instability growth mechanism to operate. Thus, the seasonal variation in the time and percentage occurrence of post midnight spread-F could partly be attributed to the MTM induced neutral wind perturbation and subsequent lowering of the F-region altitude at lower latitudes.

itudes.

Acknowledgements. The financial support from the Department of Science and Technology, Government of India and the Indian Space Research Organization is acknowledged. The SROSS C2 data is provided by Dr. S. C. Garg and Mr. P. Subrahmanyam of NPL, New Delhi.

Topical Editor M. Lester thanks a referee for his help in evaluating this paper.

References

- Abdu, M. A., Batista, I. S., and Sobral, J. H. A.: A new aspect of magnetic declination control of equatorial spread-F and F-region dynamo, *J. Geophys. Res.*, 97, 14 897–14 904, 1992.
- Chandra, H. and Rastogi, R. G.: Equatorial spread-F over a solar cycle, *Ann. Geophysicae*, 28, 37–44, 1972.
- Colerico, M., Mendillo, M., Nottingham, D., Baumgardner, J., Meriwether, J., Mirick, J., Reinish, B., Sacli, J., Fesen, C., and Biondi, M. A.: Coordinated measurements of F-region dynamics related to the thermospheric midnight temperature maximum, *J. Geophys. Res.*, 101, 26 783–26 793, 1996.
- Herrero, F. A. and Meriwether, J. W.: 6300 Å airglow meridional intensity gradients, *J. Geophys. Res.*, 85, 4191–4204, 1980.
- Herrero, F. A., Spencer, N. W., and Mayr, H. G.: Thermospheric and F-region plasma dynamics in the equatorial region, *Adv. Space Res.*, 13, 201–220, 1993.
- MacDougall, J. W., Abdu, M. A., Jayachandran, P. T., Cecile, J. F., and Batista, I. S.: Pre sunrise spread-F at Fortaleza, *J. Geophys. Res.*, 97, 13 865–13 876, 1998.
- Maruyama, T. and Matuura, N.: Longitudinal variability of annual changes in activity of equatorial spread-F and plasma bubbles, *J. Geophys. Res.*, 89, 10 903–10 912, 1984.
- Maruyama, T.: A diagnostic model for equatorial spread-F 1. Model description and application to electric field and neutral wind effects, *J. Geophys. Res.*, 93, 14 611–14 622, 1988.
- Mendillo, M., Baumgardner, J., Pi, Xiaoqing, Sultan, P. J. and, Tsunoda, R.: Onset conditions for equatorial spread-F, *J. Geophys. Res.*, 97, 13 865–13 876, 1992.
- Mendillo, M., Meriwether, J., and Biondi, M.: Testing the thermospheric neutral wind suppression mechanism for day to day variability of equatorial spread-F, *J. Geophys. Res.*, 106, 3655–3663, 2001.
- Ossakow, S. L.: Spread-F Theories – A review, *J. Atmos. Sol. Terr. Phys.*, 43, 437–452, 1981.
- Raghava Rao, R., Sekar, R., and Suhasini, R.: Nonlinear numerical simulation of equatorial spread-F – Effects of winds and electric fields, *Adv. Space Res.*, 12, 227–230, 1992.
- Sastri, J. H.: Post-midnight onset of spread-F at Kodaikanal during the June solstice of solar minimum, *Ann. Geophysicae*, 17, 1111–1115, 1999.
- Subba Rao, K. S. V. and Krishna Murthy, B. V.: Seasonal Variations of Equatorial spread-F, *Ann. Geophysicae*, 12, 33–39, 1994.